A THERMAL RESISTANCE MODEL FOR CONJUGATE HEAT TRANSFER FROM AN ISOTHERMAL CUBIC HEAT SOURCE ON A VERTICAL PLATE

By

Yelu Huang[1] and M. M. Yovanovich[2]
Microelectronics Heat Transfer Laboratory
Department of Mechanical Engineering
University of Waterloo
Waterloo, Ontario, N2L 3G1 Canada.

ABSTRACT

A simple thermal resistance model for conjugate natural convection heat transfer from an isothermal cubic heat source attached to a vertical plate is developed to predict heat source temperature and the thermal performance of the plate. The proposed model is useful in applications related to microelectronic cooling, as it can provide circuit designers with a quick estimate of the junction temperature and the effect of common design parameters due to natural convection cooling of a single chip package on printed circuit boards (PCB).

The model is based on a novel analytical-numerical method to determine various heat transfer resistances. The convection and radiation resistances from the heat source to the ambient and the contact resistance between the heat source and the plate are determined analytically. The resistances of the plate center section are obtained from an analytical solution of the 3D heat conduction equation, and the resistances of the plate fin section are obtained numerically from the solution of the discretized conduction equation. The effect of some parameters such as the plate conductivity, thickness and emissivity, and the contact resistance between the heat source and the plate are examined in detail to determine the relative merit of each as a means of improving cooling of IC packages on PCBs.

The validity and accuracy of the model is demonstrated by comparisons with experiment data and a MicroElectronic Thermal Analyser (META). An experiment is conducted in which the heat transfer from an aluminum heated cube attached to a vertical plate with or without copper layer is examined by monitoring the temperature excess of the cube. It is shown that good agreement is obtained between the experimental data and META and the prediction of the thermal resistance model.

It is found that adding high conductivity copper land on one side of the board around the heat source can reduce the heat source temperature up to 20%. The most significant

[1]Graduate Research Assistant, Presently Member of Technical Staff, Com Dev Ltd.
[2]Professor of Mechanical and Electrical Engineering, Fellow AAAS, AIAA and ASME

effect of the copper land is attributed to a very small region closest to the heat source, with increases in the size of land contributing very little to the overall cooling of the heat source. It is also shown that the effect of radiation should be included, as the radiation from the heat source surface and the entire circuit board surface may account for up to 33% and 46% of the total heat dissipation, respectively.

NOMENCLATURE

A_b	base area of cube (m^2)
A_c	total exposed surface area of cube (m^2)
A_l	plan area of copper land (m^2)
A_p	total exposed surface area of plate (m^2)
A_{si}	surface area of ith control volume of fin section (m^2)
A_t	fin tip surface area (m^2)
a	side of cube (m)
a_i, b_i, c_i, d_i	coefficients of the discretized equation
$a_{m,n}{}^*$, $b_{m,n}{}^*$	coefficients as defined in Eq. (23) and Eq. (24)
Bi	Biot number $\equiv ht/k$
Bi_b, Bi_c	dimensionless variables as defined in Eq. (30) and Eq. (29)
b	side of plate (m)
c	side of cube (m)
F_1, F_2, F_3, F_4	coefficients as defined in Eq. (25)—(28)
F_{cs}	view factor from the cube to surroundings
F_{is}	view factor from the front surface of ith control volume to surroundings
f	function
g	acceleration due to gravity (m/s^2)
h	convective coefficient $(W/m^2 \cdot K)$
h_b	total film coefficient over the back side of center section $(W/m^2 \cdot K)$
h_c	average convection coefficient over the cube $(W/m^2 \cdot K)$
h_{cc}	contact conductance $(W/m^2 \cdot K)$
h_{ci}	convection coefficient over the surface of ith control volume $(W/m^2 \cdot K)$
h_r	equivalent radiation coefficient over the cube $(W/m^2 \cdot K)$
h_{ri}	equivalent radiation coefficient over the surface of ith control volume $(W/m^2 \cdot K)$
h_{rt}	equivalent radiation coefficient over the fin tip $(W/m^2 \cdot K)$
h_t	total film coefficient over the fin tip $(W/m^2 \cdot K)$
k	thermal conductivity of plate $(W/m \cdot K)$
k_{cu}	thermal conductivity of copper layer $(W/m \cdot K)$
k_{ei}	effective thermal conductivity of ith control volume of fin section $(W/m \cdot K)$
k_f	thermal conductivity of ambient medium $(W/m \cdot K)$
L	length of copper layer around the cube (m)
N	number of control volumes
N_c	number of control volumes of the plate section with copper layer
Q	total cube heat flow rate (W)

$Q_{cp(cd)}$	heat flow rate from the cube to the plate by conduction (W)
$Q_{ca(cv)}$	heat flow rate from the cube to the ambient by convection (W)
$Q_{ca(rd)}$	heat flow rate from the cube to the ambient by radiation (W)
Q_{cc}	heat flow rate from the cube to the center section (W)
Q_{co}	heat flow rate from the cube to the fin root (W)
$Q_{pa(cv)}$	heat flow rate from the plate to the ambient by convection (W)
$Q_{pa(rd)}$	heat flow rate from the plate to the ambient by radiation (W)
Ra	Rayleigh number, dimensionless
R	total thermal resistance from the cube to the ambient $(°C/W)$
$R_{ca(cv)}$	cube to ambient convection thermal resistance $(°C/W)$
$R_{ca(rd)}$	cube to ambient radiation thermal resistance $(°C/W)$
R_{cc}	cube to center section heat dissipation Q_{cc} thermal resistance $(°C/W)$
R_{co}	cube to fin root heat dissipation Q_{co} thermal resistance $(°C/W)$
R_f	fin section thermal resistance $(°C/W)$
$R_{ia(cv)}$	ith control volume to ambient convection thermal resistance $(°C/W)$
$R_{ia(rd)}$	ith control volume to ambient radiation thermal resistance $(°C/W)$
$R_{ij(cd)}$	conduction thermal resistance between ith and jth control volumes $(°C/W)$
T	temperature of center section $(°C)$
T_c	cube temperature or mean package case temperature $(°C)$
T_f	local ambient mean temperature or surrounding temperature $(°C)$
T_i	average temperature of ith control volume of fin section $(°C)$
T_o	root temperature of fin section $(°C)$
t	plate thickness (m)
t_{cu}	copper layer thickness (m)
X, Y, Z	cartesian coordinates

Greek Symbols

α	thermal diffusivity (m^2/s)
β	expansion coefficient of air $(1/K)$
ν	kinematic viscosity of air (m^2/s)
ΔT_c	temperature difference between cube and ambient $(°C)$
ϵ_c	cube surface emissivity
ϵ_{cu}	copper layer surface emissivity
ϵ_p	plate surface emissivity
ϵ_{pi}	plate ith control volume surface emissivity
ε_m, λ_n	separation constants
$\gamma_{m,n}$	effective separation constant
σ	Stefan-Boltzmann constant $(W/m^2 \cdot K^4)$
θ_c	cube temperature rise above the root temperature $\equiv T_c - T_o$, $°C$
θ_f	fluid temperature rise above the root temperature $\equiv T_f - T_o$, $°C$

Subscripts

$\sqrt{A}$	using $\sqrt{A}$ as the characteristic length
m, n	series indices on coefficients
$\overline{cf}$	using mean temperature $\frac{1}{2}(T_c + T_f)$ for properties calculation
$\overline{if}$	using mean temperature $\frac{1}{2}(T_i + T_f)$ for properties calculation

INTRODUCTION

The thermal design of microelectronic equipment has assumed a more prominent role in recent years due to the trend towards increased component packaging densities and high powered integrated circuits. Reliability considerations of silicon based devices require that chip junction temperature not exceed a maximum value of $85°C$ to $125°C$ depending upon on the application [1]. Thus, it is necessary to predict and control operating chip temperatures to ensure reliability within electronic systems. In addition, during the early stages of the design process, the circuit designer is primarily concerned with determining the sensitivity of junction temperatures to changes in basic printed circuit board (PCB) parameters over which the circuit designer has some control.

Recent years have witnessed a proliferation in the use of junction to ambient thermal resistance (R_{ja}) for the thermal characterization of packages. Unfortunately, as noted by Andrews [2] and Bar-Cohen et al. [3], a specific R_{ja} value will not adequately reflect the dependence of package thermal performance in the actual operating environment. It is necessary to combine with the PCB model to determine the actual temperatures of the package. Various PCB models have been developed , most of which analyze heat transfer and temperature distribution of PCBs by assuming chips, or other heat sources flushed mounted on the board. Culham et al. [4] incorporated a detailed package model developed by Lemczyk et al. [5] within a PCB model, MicroElectronic Thermal Analyser, called META to allow internal package thermal resistances to be determined and give a detailed thermal description for each package with junction temperature.

A few recent studies, notably those of Culham and Yovanovich [6], Graham and Witzman [7], Laderman, et al. [8] and S. Lee, et al. [9] have addressed the parameter studies of PCBs on the cooling of electronic packages mounted on the board. Culham and Yovanovich [6] used a one-dimensional analytical/numerical model to determine the effects of some PCB parameters. Graham and Witzman [7] presented an analytical expression, supplemented with experimental data to correlate the junction temperature of a convectively cooled single-component package mounted on a PCB to a number of factors which include the component package size and PCB characteristics. But the above analyses are limited to the thermal conductivity, the thickness of the PCB and the forced convection film coefficient. Laderman et al. [8] used the SINDA computer program to provide a parametric study to determine the relative effectiveness of various conduction heat transfer schemes for cooling of a typical high power density SMT package on a multilayer PCB. The analysis was limited to conduction cooling and also the PCB was assumed to be connected to the cooled wall which acted as a uniform temperature heat sink. Lee et al. [9] used META to predict the effect of some design parameters on the thermal performance of microelectronic equipment. As META neglects the temperature gradient across the thickness of the board, the effect of the PCB thickness was not considered.

So far no work has been found which uses a simple thermal resistance network to predict the junction temperature and to analyze the effect of basic design parameters of the PCB on the natural convection cooling of electronic package. It is to this end that a simple thermal resistance model for conjugate natural convection heat transfer from an electronic

package/circuit board prototype consisting of an isothermal cubic heat source attached to a vertical plate was developed.

THERMAL RESISTANCE MODEL

Model Assumptions

In order to simplify the problem, but retain the nature of the physics, the following assumptions are made in the present research:

1. As shown in Fig. 1, the single chip package is modelled as an isothermal cube, and attached to the center of the board with the contact conductance h_{cc}.

2. The circuit board is suspended in a quiescent fluid which is contained within surroundings of large extent. The fluid and the surroundings are maintained at a uniform temperature T_f.

3. The printed circuit board is assumed as a square homogeneous plate with a copper layer attached to one side. The copper layer is attached around the cube with the same length L ($L = c - a$). The exposed area of the copper layer around the cube, denoted as A_l, can be related to the base area of the cube A_b to provide a convenient measure of the size of the copper land.

4. The plate is divided into two sections, the fin section and the center section, as shown in Fig. 1. Although the convective heat transfer coefficient varies significantly over the surfaces of the fin section, typical values of the Biot Number ($Bi \equiv$ht/k) range from 0.0003 to 0.1. Therefore the temperature gradient across the thickness of the fin section will be neglected. It is noted that this assumption will not be used for the center section due to the high contact conductance h_{cc} on one of its surfaces.

5. The fin section is discretized into N control volumes, as shown in Fig. 2. The continuous variation of temperature of this section is modelled by determining the values at discrete points located at the center of each control volume.

6. The emissivity of the plate, the copper layer, and the cube are assumed uniform.

General Resistance Equation

Figure 3 shows the heat transfer paths from the cube. The total heat Q dissipated in the cube is removed by convection $Q_{ca(cv)}$, radiation $Q_{ca(rd)}$ from the cube surface area and conduction $Q_{cp(cd)}$ to the plate through the contact area between the cube and the plate. $Q_{cp(cd)}$ consists of two parts Q_{cc} and Q_{co}, where Q_{cc} is conducted through the thickness of the center section and then removed by convection and radiation to the surrounding air medium; Q_{co} conducts along the plate in the X, Y directions, and is finally removed by convection and radiation from the surface of the fin section. Therefore one has the thermal resistance

network of a cube on plate assembly as shown in Fig. 4. The total thermal resistance is:

$$R = \left(\frac{1}{R_{ca(rd)}} + \frac{1}{R_{ca(cv)}} + \frac{1}{R_{cc}} + \frac{1}{R_{co} + R_f}\right)^{-1} \tag{1}$$

where the overall resistance and the component resistances are defined as:

$$R = \frac{T_c - T_f}{Q} \tag{2}$$

$$R_{ca(cv)} = \frac{T_c - T_f}{Q_{ca(cv)}} = \frac{1}{h_c A_c} \tag{3}$$

$$R_{ca(rd)} = \frac{T_c - T_f}{Q_{ca(rd)}} = \frac{1}{h_r A_c} \tag{4}$$

$$R_{cc} = \frac{T_c - T_f}{Q_{cc}} \tag{5}$$

$$R_{co} = \frac{T_c - T_o}{Q_{co}} \tag{6}$$

$$R_f = \frac{T_o - T_f}{Q_{co}} \tag{7}$$

Convection and Radiation Resistances of the Cube

$R_{ca(cv)}$ and $R_{ca(rd)}$ are the convection and radiation resistances of the cube to the ambient respectively. They are determined by average convection and equivalent radiation coefficients h_c and h_r over the cube respectively. For the present study, h_c is approximated by using the correlation of Yovanovich [10] for an isothermal cube in natural convection, and h_r is calculated by approximating the system as a two surface enclosure with small convex object (cube-on-plate) in a large cavity (surroundings) [11], they are:

$$h_c = \frac{3.388 + 0.489(Ra_{\sqrt{A_c}})^{\frac{1}{4}} k_{f_{\overline{cf}}}}{\sqrt{A_c}} \tag{8}$$

where the Rayleigh number is defined as

$$Ra_{\sqrt{A_c}} = \left(\frac{g\beta}{\nu\alpha}\right)_{\overline{cf}} (T_c - T_f)\left(\sqrt{A_c}\right)^3 \tag{9}$$

The air property values $\left(\frac{g\beta}{\nu\alpha}\right)_{\overline{cf}}$, $k_{f_{\overline{cf}}}$ are obtained from dry air correlations given in [11], and the subscript $\overline{cf}$ denotes that the mean temperature $\frac{1}{2}(T_c + T_f)$ is used for the air properties calculations.

$$h_r = \frac{F_{cs}\epsilon_c\sigma\left[(T_c + 273)^4 - (T_f + 273)^4\right]}{T_c - T_f} \tag{10}$$

F_{cs} is the radiation view factor from the cube to the surroundings, which is found to be 0.696 [11].

Center Section Analytical Solution

R_{cc} and R_{co} are the resistances for Q_{cc} and Q_{co} respectively. It is important to note that both R_{cc} and R_{co} inherently include contact resistance between the cube and the plate. Besides, R_{cc} includes the conduction resistance of the center section in the Z direction and convection and radiation resistances on the back side of the center section. R_{co} includes the conduction resistance of the center section in the X and Y directions. Q_{cc} and Q_{co} can be obtained from the solution of the three-dimensional heat conduction equation in the center section if the average root temperature T_o, and the average film coefficient around the back side of center section h_b are assumed known. Figure 5 shows the configuration and the assumed boundary conditions of the center section. It is important to note that the assumed boundary conditions of T_o and h_b can be determined later by solving the entire thermal resistance network through an iterative procedure. Due to configuration symmetry, it is only necessary to model a quarter of this center section. The conduction equation:

$$\frac{\partial^2 T}{\partial x^2} + \frac{\partial^2 T}{\partial y^2} + \frac{\partial^2 T}{\partial z^2} = 0 \tag{11}$$

with the boundary conditions:

$$x = 0 \qquad T = T_o \tag{12}$$

$$x = a \qquad \frac{\partial T}{\partial x} = 0 \tag{13}$$

$$y = 0 \qquad T = T_o \tag{14}$$

$$y = a \qquad \frac{\partial T}{\partial y} = 0 \tag{15}$$

$$z = 0 \quad k\frac{\partial T}{\partial z} - h_b(T - T_f) = 0 \tag{16}$$

$$z = t \quad k\frac{\partial T}{\partial z} + h_{cc}(T - T_c) = 0 \tag{17}$$

A separable solution to Eq. (11) subject to boundary conditions, Eqs. (12)—(17) can be formed in a straightforward manner [11]. So finally Q_{cc} and Q_{co} can be found as:

$$Q_{cc} = ka \sum_{m=1}^{\infty} \sum_{n=1}^{\infty} \frac{\gamma_{m,n}}{\varepsilon_m \lambda_n} b^*_{m,n} \cosh^{-1}\left(\frac{\gamma_{m,n} t}{a}\right) \tag{18}$$

and

$$Q_{co} = ka \sum_{m=1}^{\infty} \sum_{n=1}^{\infty} \frac{\gamma_{m,n}}{\varepsilon_m \lambda_n} \left\{ a^*_{m,n} \tanh\left(\frac{\gamma_{m,n} t}{a}\right) + b^*_{m,n} \left[1 - \cosh^{-1}\left(\frac{\gamma_{m,n} t}{a}\right)\right] \right\} \tag{19}$$

where the separation constants and other system parameters are defined below:

$$\varepsilon_m = (m - \frac{1}{2})\pi \tag{20}$$

$$\lambda_n = (n - \frac{1}{2})\pi \tag{21}$$

$$\gamma_{m,n} = \sqrt{\varepsilon_m^2 + \lambda_n^2} \tag{22}$$

$$a^*_{m,n} = (F_1 + F_2F_3)^{-1}(\frac{4Bi_c\theta_c}{\varepsilon_m\lambda_n} - F_2F_4) \quad (23)$$

$$b^*_{m,n} = \frac{F_3}{F_1 + F_2F_3}(\frac{4Bi_c\theta_c}{\varepsilon_m\lambda_n} - F_2F_4) + F_4 \quad (24)$$

$$F_1 = Bi_c + \gamma_{m,n}\tanh(\frac{\gamma_{m,n}t}{a}) \quad (25)$$

$$F_2 = \gamma_{m,n} + Bi_c\tanh(\frac{\gamma_{m,n}t}{a}) \quad (26)$$

$$F_3 = \frac{Bi_b}{\gamma_{m,n}} \quad (27)$$

$$F_4 = -\frac{4\cosh(\frac{\gamma_{m,n}t}{a})Bi_b\theta_f}{\gamma_{m,n}\varepsilon_m\lambda_n} \quad (28)$$

$$Bi_c = \frac{h_{cc}a}{k} \quad (29)$$

$$Bi_b = \frac{h_ba}{k} \quad (30)$$

$$\theta_c = T_c - T_o \quad (31)$$

$$\theta_f = T_f - T_o \quad (32)$$

Th numerical results of Q_{cc} and Q_{co} were obtained using $M = 20$ terms as the Fourier Series Truncation Limit. This was found to converge temperatures to within 4.5%.

Fin Section Numerical Solution

1. Temperature Discretization Equation

R_f is the total resistance of the fin section which includes the conduction resistance through the fin and the convection and radiation resistances on the surface of the fin section. Discretizing the fin section into N control volumes and performing an energy balance on the different control volumes as shown in Fig. 2, one obtains the discretized equation:

$$a_iT_i = b_iT_{i-1} + c_iT_{i+1} + d_i \quad (33)$$

where:

$$a_i = \begin{cases} b_i + c_i + (h_{ci} + h_{ri})r_i\Delta r_i + \frac{k_{ei}tr_i}{\Delta r_i} & \text{if } i = 1 \\ b_i + c_i + \frac{d_i}{T_f} & \text{if } i \neq 1 \end{cases} \quad (34)$$

$$b_i = \begin{cases} 0 & \text{if } i = 1 \\ \frac{k_{ei}r_it}{\Delta r_i + \Delta r_{i-1}} & \text{if } i \neq 1 \end{cases} \quad (35)$$

$$c_i = \begin{cases} 0 & \text{if } i = N \\ \frac{k_{ei}t(r_i + \Delta r_i)}{\Delta r_i + \Delta r_{i+1}} & \text{if } i \neq N \end{cases} \quad (36)$$

$$d_i = \begin{cases} (h_{ci}+h_{ri})r_i\Delta r_i T_f + \dfrac{k_{ei}tr_i}{\Delta r_i}T_o & \text{if } i=1 \\ (h_{ci}+h_{ri})r_i\Delta r_i T_f + \frac{1}{2}h_t(r_i+\Delta r_i)tT_f & \text{if } i=N \\ (h_{ci}+h_{ri})r_i\Delta r_i T_f & \text{if } i\neq 1 \text{ and } i\neq N \end{cases} \tag{37}$$

The discrete convection, equivalent radiation coefficients, and surface emissivities and conductivities are calculated by means of the equations given below:

$$h_{ci} = \frac{\left\{3.21+0.559(Ra_{\sqrt{A_p}})^{\frac{1}{4}}\right\}k_{f_{\overline{if}}}}{\sqrt{A_p}} \tag{38}$$

$$h_{ri} = \frac{\frac{F_{is}+1}{2}\epsilon_{pi}\sigma\left[(T_i+273)^4-(T_f+273)^4\right]}{T_i-T_f} \tag{39}$$

$$\begin{aligned} h_t &= h_{cN}+h_{rt} \\ &= h_{cN}+\frac{\epsilon_p\sigma\left[(T_N+273)^4-(T_f+273)^4\right]}{T_N-T_f} \end{aligned} \tag{40}$$

$$\epsilon_{pi} = \begin{cases} \epsilon_{cu} & \text{if } i\leq N_c \\ \epsilon_p & \text{if } i>N_c \end{cases} \tag{41}$$

$$k_{ei} = \begin{cases} k+k_{cu}\dfrac{t_{cu}}{t} & \text{if } i\leq N_c \\ k & \text{if } i>N_c \end{cases} \tag{42}$$

It is noted that correlations of Yovanovich [10] and Lee et al. [12] for an isothermal vertical plate in natural convection are used to approximate the average convection coefficient h_{ci} over the surface of ith control volume, and Eq. (9) is used to define $Ra_{\sqrt{A_p}}$ with the difference that T_i and A_p are used instead of T_c and A_c respectively. A similar method is used to approximate the equivalent radiation coefficient h_{ri} over the surface of the ith control volume. h_t is the combined convection and radiation coefficient of the fin tip. The calculation of the radiation view factor F_{is} from the front surface of ith control volume to surroundings can be found in [11]. Equation (33) can be solved using the TDMA method [13].

2. Computation of Component Resistances

The fin section component resistances can be determined from the following steps:

$$R_{ia(cv)} = \begin{cases} \dfrac{1}{h_{ci}A_{si}} & \text{if } i\neq N \\ \dfrac{1}{h_{ci}(A_{si}+A_t)} & \text{if } i=N \end{cases} \tag{43}$$

$$R_{ia(rd)} = \begin{cases} \dfrac{1}{h_{ri}A_{si}} & \text{if } i\neq N \\ \dfrac{1}{h_{ri}A_{si}+h_{rt}A_t} & \text{if } i=N \end{cases} \tag{44}$$

$$R_{o1(cd)} = \frac{T_o-T_1}{(h_{c1}+h_{r1})(T_1-T_f)A_{s1}+\dfrac{T_1-T_2}{R_{12(cd)}}} \tag{45}$$

$$R_{12(cd)} = \frac{T_1 - T_2}{(h_{c2} + h_{r2})(T_2 - T_f) A_{s2} + \dfrac{T_2 - T_3}{R_{23(cd)}}} \tag{46}$$

$$\vdots$$

$$R_{N-1N(cd)} = \frac{T_{N-1} - T_N}{(h_{cN} + h_{rN}) A_{sN} + h_t A_t (T_N - T_f)} \tag{47}$$

3. Computation of Fin Resistance

The fin section resistance R_f can be determined from the following steps:

$$R_f = R_{f1} \tag{48}$$

$$R_{f1} = R_{o1(cd)} + \frac{1}{\dfrac{1}{R_{1a(rd)}} + \dfrac{1}{R_{1a(cv)}} + \dfrac{1}{R_{f2}}} \tag{49}$$

$$R_{f2} = R_{12(cd)} + \frac{1}{\dfrac{1}{R_{2a(rd)}} + \dfrac{1}{R_{2a(cv)}} + \dfrac{1}{R_{f3}}} \tag{50}$$

$$R_{f3} = R_{23(cd)} + \frac{1}{\dfrac{1}{R_{3a(rd)}} + \dfrac{1}{R_{3a(cv)}} + \dfrac{1}{R_{f4}}} \tag{51}$$

$$\vdots$$

$$R_{fN} = R_{N-1N(cd)} + \frac{1}{\dfrac{1}{R_{Na(rd)}} + \dfrac{1}{R_{Na(cv)}}} \tag{52}$$

The above procedure shows that a novel analytical-numerical method is used to determine various heat transfer resistances. Substituting the above resistance calculation equations into the general resistance equation, Eq. (1), one can calculate the temperature of the cube which is related to several parameters as given by the following relationship:

$$T_c = f(Q, T_f, h_{cc}, k, k_{cu}, \epsilon_p, \epsilon_{cu}, \epsilon_c, a, b, c, t, t_{cu}) \tag{53}$$

Therefore, if the total power dissipation and the physical and geometrical parameters are known, the cube temperature can be determined. It is noted that these resistances are nonlinear due to their dependencies on cube temperature T_c. Therefore an iterative procedure is required to calculate these resistances and finally one can determine the cube temperature T_c [11]. Usually 7 to 8 iteration are required for the convergence criterion set on the cube temperature. The details of determining the convergence criterion can be found in [11].

MODEL RESULTS AND DISCUSSION

The following presents several parametric studies using the proposed thermal resistance model. The sensitivity of the cubic heat source temperature excess $\Delta T_c = T_c - T_f$ with

respect to some parameters such as the plate conductivity, thickness and emissivity, and the contact resistance between the heat source and the plate are examined in detail to determine the relative merit of each as a means of improving cooling of IC packages attached to PCBs.

Except as indicated otherwise, the result for each parametric study is obtained by varying only the parameter of interest such as plate thermal conductivity, thickness, and emissivity, etc, while maintaining all other design parameters at the default values, which are given in the following:

plate parameters:	$b = 228.6\ mm$
	$t = 1.5\ mm$
	$k = 2\ W/m \cdot K$
	$\epsilon_p = 0.1$
cube parameters:	$a = 43.26\ mm$
	$\epsilon_c = 0.085$
	$Q = 5\ W$
	$h_{cc} = 10^5\ W/m \cdot K$
copper layer parameters	$L = 0\ mm$
	$k_{cu} = 386\ W/m \cdot K$
	$t_{cu} = 0.0343\ mm$
	$\epsilon_{cu} = 0.06$
fluid and ambient temperatures:	$T_f = 293\ K$

Effect of Plate Thermal Conductivity

The effect of plate thermal conductivity on the heat source temperature reduction is shown in Fig. 6 for three power levels. It is seen that the cube temperature excess is strongly affected by the thermal conductivity of the plate, and increasing the thermal conductivity spreads the heat in the plate more easily which results in lower cube temperatures. This shows the advantage of incorporating high conductivity materials like copper in the PCB. The gains are, however, limited as can be seen in Fig. 6, where the cube temperature excess is negligible after the plate conductivity becomes larger than about 100W/m·K for the cases analyzed here. This is because the plate is approaching an isothermal condition beyond which increasing its thermal conductivity has negligible effect on the heat source temperature excess. Figure 6 also reveals that the most significant reduction of cube temperature occurs between a thermal conductivity of 1 and 10W/m·K, where a tenfold increase in thermal conductivity from 1—10W/m·K results in more than 40% reduction of the cube temperature. This phenomenon is quite similar with that observed by Culham and Yovanovich [6]. Coincidentally, the conductivity of 1—10W/m·K is the range of board thermal conductivities observed in most fiber/copper PCBs. Therefore a small increase of copper content in the PCB can significantly reduce the heat source temperature excess.

Effect of Copper Layer

To examine the effect of copper layer on the cube temperature excess, four different lengths of copper layer: $L = 0.0$ (default case), $L = (b-a)/4$, $L = (b-a)/2$, and $L = b-a$, corresponding to $A_l/A_c = 0.0$, $A_l/A_c = 3.3$, $A_l/A_c = 8.9$, and $A_l/A_c = 27.0$ were studied in detail. The results with change of the plate conductivity are shown in Fig. 7. It is shown that adding high conductivity copper land on one side of the board around the heat source can reduce the heat source temperature up to 20%. The most significant effect of the copper layer is attributed to a small region closest to the heat source ($A_l/A_c \leq 3.3$), with increase in the size of the copper layer contributing very little to the overall cooling of the heat source. Figure 7 also reveals that the most significant effect of copper layer occurs when the plate conductivity is about 1W/m·K. It is expected that there is almost no contribution of the copper layer on the overall cooling of the heat source as the thermal conductivity approaches 100W/m·K.

Effect of Plate Thickness

A typical single layer board has a thickness of slightly less than 2 mm, while some multilayer boards may approach a thickness of 4 mm. The effect on the cube temperature due to varying thickness over this range of values is shown in Fig. 8, where the cube temperature excess is plotted against the plate thermal conductivity. It is clearly shown that a thicker plate results in lower cube temperature for the cases examined here. This occurs because the heat flux spreads more easily in the thicker plate. Figure 8 also reveals that the most significant effect of plate thickness occurs when the plate conductivity is around 10W/m·K.

Effect of Plate Emissivity

The effect of plate surface emissivity is shown in Fig. 9. It is evident that an increase in plate emissivity results in a decrease in cube temperature. This is because more heat will be dissipated from the surface of the plate by radiation as the surface emissivity increases. Figure 9 also reveals that the cube temperature excess reduction various almost linearly with the plate emissivity over the examined range of plate thermal conductivity.

Effect of Contact Resistance between Cube and Plate

The effect of thermal contact resistance on the cube temperature was examined by assuming different values of thermal contact conductance, and the results are shown in Fig. 10. It is evident that higher contact conductance (lower contact resistance) results in lower cube temperatures, since more heat will be dissipated to the plate from the cube by conduction as the contact conductance increases. But there is a limit, when the contact conductance is increased beyond 10^4W/m·K, the decrease in the cube temperature excess is negligible. Therefore, a perfect contact condition can be defined approximately by assuming $h_{cc} \geq 10^4$W/m·K. In the present study, h_{cc} is assumed to be 10^5W/m·K for a perfect contact condition. Also Fig. 10 shows that the effect of contact resistance will be more significant for higher plate conductivities. This is because plates with higher conductivities will provide the dominant heat transfer path by conduction, therefore the plate resistance which includes contact resistance in the proposed model will have a larger effect on the reduction of heat source temperature. When the plate conductivity is less than 0.1W/m·K, the effect of contact resistance is negligible.

Summary of the Fraction of Heat Dissipation

As mentioned previously, the total heat Q dissipated in the cube is removed by convection $Q_{ca(cv)}$, radiation $Q_{ca(rd)}$ from the cube surface area and conduction $Q_{cp(cd)}$ to the plate through the contact area between the cube and the plate. Figure 11 summarizes the relative fraction of heat dissipation attributed to each of the three modes of heat transfer from the heat source for the default case (except for the value of ϵ_c as indicated in the figure). It can be seen that when the thermal conductivity is larger than 3W/m·K, conduction is the predominant mode of heat dissipation from the source. As the plate conductivity decreases, less heat is conducted away from the heat source through the plate and more heat has to be dissipated directly into the ambient through the surface of the source by convection and radiation. However for small conductivity(e.g., k=0.1W/m·K), conduction still accounts for approximately 18% of the total heat transfer. So conduction heat transfer through the plate must be considered even for low conductivity materials, such as plastics and fiberglass found in most circuit board constructions. Figure 11 also shows the change in heat dissipation due to conduction, convection and radiation for changes in the surface emissivity of the heat source. When the heat source emissivity is increased, the component of heat previously dissipated by conduction and convection is dissipated by radiation. For most fiber PCBs, the conductivities of which are around 1—10W/m·K, the radiation may account for up to 33% of the total heat dissipation from the heat source. As can be seen from the figure, when $\epsilon_c = 1$, the magnitude of radiation loss is comparable to that of convection.

The conduction dissipation $Q_{cp(cd)}$ from the cube is dissipated through the plate and it is finally removed by convection $Q_{pa(cv)}$ and radiation $Q_{pa(rd)}$ from the exposed surface of the plate. Figure 12 summarizes the relative fraction of heat dissipation from the plate due to convection and radiation for the default case (except the value of ϵ_p as indicated in the figure). As the plate conductivity increases, more heat is conducted away from the heat source through the plate, which is finally dissipated through the surface of the plate by radiation and convection. For the plate conductivity range of 1–10W/m·K, the radiation heat loss from the plate may account for up to 46% of the total heat dissipation.

COMPARISON WITH EXPERIMENTAL RESULTS AND META

To verify the thermal resistance model (TRM), a series of experiments are conducted in which the significance of conjugate heat transfer, including conduction, natural convection and radiation from an aluminum heated cube attached to a vertical plate is studied by monitoring temperatures in the cube and the surrounding air medium. All tests are performed under steady state conditions and limited to natural convection over a range of Rayleigh numbers between 5.4 $\times 10^5$ to 6.7 $\times 10^6$, where the characteristic length of the Rayleigh number is based on the square root of the exposed surface area of the cube.

The dimensions and thermophysical properties of the aluminum cube are maintained in each experiment while the internal thermal resistance of the plate is altered by varying the plate conductivity, thickness, and emissivity. For the cube on the plate without copper layer tests, cubes on three homogeneous plates made of plexiglass, stainless steel and copper,

Table 1: Plate dimensions, thermal conductivity and surface emissivity of each test case.

Case	Plate	Length (mm)	Width (mm)	Thickness (mm)	Conductivity $(W/m \cdot K)$	Emissivity
1A	plexiglas	228.6	228.6	3.2	0.19[14]	0.90
1B	304 SS polished	228.6	228.6	1.5	13.4[14]	0.14
1C	copper	228.6	228.6	1.6	401[15]	0.03–0.06

Table 2: The copper land specifications for each cases [11].

Case	Copper Land	Length (mm)	Width (mm)	Thickness (mm)	Conductivity $(W/m \cdot K)$	Emissivity
2A	$A_l/A_c = 27.0$	92.7	92.7	0.0343	386	0.06
2B	$A_l/A_c = 8.9$	46.4	46.4	0.0343	386	0.06
2C	$A_l/A_c = 3.6$	25.0	25.0	0.0343	386	0.06
2D	$A_l/A_c = 0.0$	0	0	0	–	–

Table 3: Experimental vs. TRM and META predicted ΔT_c for case 1B.

	$h_{cc} = 500 W/m^2 \cdot K$		$h_{cc} = 3000 W/m^2 \cdot K$		$h_{cc} = 10^5 W/m^2 \cdot K$	
EXP	TRM	META	TRM	META	TRM	META
31.3	34.4	33.3	31.0	30.0	30.0	29.0
27.2	29.3	28.4	26.4	25.6	25.2	24.8
22.3	23.9	23.2	21.6	20.9	20.6	20.3
17.2	18.5	17.9	16.7	16.2	16.2	15.9
12.1	13.0	12.4	11.7	11.2	11.2	10.9
6.4	6.9	6.6	6.3	6.0	6.0	5.8

denoted as case 1A (Measured by Mack [14]), 1B, and 1C respectively were examined. Table 1 summarizes the plate dimensions, thermal conductivities and surface emissivities for each case.

In addition to using homogeneous plates, a fiberglass reinforced epoxy plate (FR4) with a one ounce layer of copper attached to one side is used. The conductivity, thickness and emissivity of the FR4 plate without copper layer are 0.41W/m·K, 15.9 mm and 0.9 respectively [11]. The experiment is initiated by testing the plate with fully covered copper layer on one side ($A_l/A_c = 27.0$). Further tests were conducted for cases where the copper layer closest to the edge of the plate was progressively etched away by using PC etch solution and etch resistance solution. The plan dimensions of all plates are still maintained at 228.6 $mm \times 228.6\ mm$. Table 2 presents the copper land specifications for those tests.

The experiment results are presented in terms of the cube temperature excess $\Delta T_c = T_c - T_f$ and the heat power input Q, where the cube temperature T_c is the average value of four thermocouples located in the cube, the ambient temperature T_f is the average value of three thermocouples located in the test section. Figure 13 show the experiment results for cases 1A, 1B, 1C and the predicted results of the thermal resistance model (TRM) with the assumption of contact conductances: $h_{cc} = 10^3 W/m^2 \cdot K$, $3 \times 10^3 W/m^2 \cdot K$, $10^5 W/m^2 \cdot K$, which translate into contact resistances: $1.9°C/W$, $0.2°C/W$, $0.0°C/W$ respectively. Although a conductive grease has been applied between the cube and the plate, the contact resistance still can not be neglected. Figure 13 shows that if a contact conductance $h_{cc} = 3 \times 10^3 W/m^2 \cdot K$ is assumed, there is good agreement between the experimental data and the predictions of the model. For these three cases, the absolute and percentage temperature difference are less than $0.9°C$ and 5.1% respectively [11].

Figure 14 shows the experimental results of cases 2A—2D and the predicted results of the model with the assumption of contact conductance $h_{cc} = 3 \times 10^3 W/m^2 \cdot K$ respectively. The absolute and percentage temperature difference for these four cases are less than $2.3°C$ and 6.4% respectively [11]. The experiments clearly verify that adding only a small amount of copper layer (A_l/A_c=3.6) on one side of the plate can reduce the cube temperature significantly ($9°C$–10 $°C$). However, the addition of more copper lands (e.g., A_l/A_c=8.9, A_l/A_c=27.0) does not significantly contribute to heat dissipation through the plate and lands.

The validity and accuracy of the model is also demonstrated by comparisons with the predictions of the MicroElectronic Thermal Analyser (META), an analytical-numerical model for air cooling of circuit boards with arbitrarily located heat sources [4]. Tables 3—4 show the predicted results of the thermal resistance model (TRM) and META for cases 1B and 2B with the assumption of contact conductance $h_{cc} = 10^3 W/m^2 \cdot K$, $3 \times 10^3 W/m^2 \cdot K$, $10^5 W/m^2 \cdot K$. It is seen that although different methods are used to calculate the conjugate heat transfer from the cube on a vertical plate, there is not much difference between the predictions of META and those of the thermal resistance model (TRM). The maximum temperature difference for cases 1B—1C, and 2A—2D is $5.9°C$, and the average temperature difference is $1.5°C$ [11].

Table 4: Experimental vs. TRM and META predicted ΔT_c for case 2B.

	$h_{cc} = 500 W/m^2 \cdot K$		$h_{cc} = 3000 W/m^2 \cdot K$		$h_{cc} = 10^5 W/m^2 \cdot K$	
EXP	TRM	META	TRM	META	TRM	META
48.5	51.3	47.9	47.7	44.7	46.6	44.0
42.3	44.4	41.6	41.3	38.8	40.3	38.2
35.5	37.3	35.0	34.6	32.7	33.8	32.2
28.5	29.8	28.0	27.6	26.2	26.9	25.9
21.3	22.2	20.9	20.5	19.6	20.0	19.3
13.5	14.2	13.5	13.1	12.7	12.7	12.5
5.0	5.2	5.0	4.8	4.8	4.7	4.7

CONCLUDING REMARKS

A simple thermal resistance model for conjugate heat transfer from an isothermal cubic heat source attached to a vertical plate can be used to predict accurately heat source temperature and the thermal performance of the plate.

The thermal conductivity of the board is the most important design parameter for reducing heat source temperature. Adding high conductivity copper land on one side of the board around the heat source can reduce the heat source temperature up to 20%. The most significant effect of the copper land is attributed to a very small region closest to the heat source, and further increases in the size of land contributes very little to the overall cooling of the heat source. Also, the most significant effect of the copper land occurs when the board thermal conductivity is around 1W/m·K or the contact resistance between the package and board is relatively low.

In addition, increasing the board thickness, emissivity or reducing the contact resistance between the package and the board will reduce the heat source temperature. Especially, for natural convection cooling where convection and radiation are of equal magnitude, the effect of radiation should be included as the radiation from the heat source surface and the entire circuit board surface may account for up to 33% and 46% of the total heat dissipation respectively.

The heat transfer coefficients determined from the correlations of Yovanovich [10] and Lee et al. [12] for the isothermal cube and plate can be successfully used for the cube on plate assembly. This makes the resistance model simple, as it does not need to solve the

momentum and energy equation in fluid side for natural convection heat transfer.

ACKNOWLEDGEMENTS

The authors wish to thank the Manufacturing Research Corporation of Ontario (MRCO) for partial support of the research project, and Bell–Northern Research (BNR) for the test PCBs.

REFERENCES

1. Kraus, A.D. and Bar-Cohen, A., *Thermal Analysis and Control of Electronic Equipment*, Hemisphere Publishing Corporation, 1983.

2. Andrews, J.A., "Thermal Resistance Model Dependency on Equipment Design," *IEEE CHMT Transactions*, 1988, Vol. CHMT-11, No. 4, pp. 528-527.

3. Bar-Cohen, A., Elperin, T., and Eliasi, R., "Θ_{jc} Characterization of Chip Packages - Justification, Limitations and Future," *IEEE Transactions on Components, Hybrids and Manufacturing Technology*, 1989, Vol. 12, No. 4, pp 724-731.

4. Culham, J.R., Lemczyk, T.F., Lee, S., and Yovanovich, M.M., "META - A Conjugate Heat Transfer Model for Air Cooling of Circuit Boards with Arbitrarily Located Heat Sources," *Heat Transfer in Electronic Equipment*, ASME HTD-Vol. 171, pp. 117-126.

5. Lemczyk, T.F., Culham, J.R. and Yovanovich, M.M., "Thermal Analysis of Microelectronic Package," *ASME Winter Annual Meeting December 1–6, 1991, Atlanta, Georgia*, Paper No. 91-WA-EEP-46.

6. Culham, J.R., and Yonvanovich, M.M., "Non-Iterative Technique for Computing Temperature Distributions in Flat Plates with Distributed Heat Sources and Convective Cooling," *Second ASME-JSME Thermal Engineering Joint Conference*, March 22–27, 1987, Honolulu, Hawaii, pp. 403–409.

7. Graham, K., and Witzman, S., 1988, "Analytical Correlation of Thermal Design of Electronic Packages," *Cooling Technology for Electronic Equipment*, (W. Aung, ed), pp. 249-264.

8. Laderman, A.J., Osborn, D.B., Grabow, R.M., and Bury, M.C., "Parametric Study of Conduction Cooling for High Power Density Electronics," *Proc. Intl. Symp. on Cooling Technology for Electronic Equipment*, 1987, Honolulu, HI, March, pp. 404–422.

9. Lee, S., Culham, J.R., and Yovanovich, M.M., "The Effect of Common Design Parameters on the Thermal Performance of Microelectronic Equipment: Part 1 – Natural Convection," *Heat Transfer in Electronic Equipment*, ASME 1991, HTD-Vol. 171, pp. 47–54.

10. Yovanovich, M.M., "On the Effect of Shape, Aspect Ratio and Orientation Upon Natural Convection from Isothermal Bodies of Complex Shape," *Convective Transport*, 1987, ASME HTD-Vol. 82, Boston, Mass., pp 121-129.

11. Huang Y., 1993, "A Thermal Resistance Model for Conjugate Heat Transfer from an Isothermal Cubic Heat Source on a Vertical Plate," M.A.Sc. Thesis, University of Waterloo, Waterloo, Canada.

12. Lee, S., Yovanovich, M.M., Jafarpur, K., "Effects of Geometry and Orientation on Laminar Natural Convection from Isothermal Bodies", *Journal of Thermophysics and Heat Transfer*, 1991, Vol.5, No.2, pp. 208–216.

13. Patankar, S.V., *Numerical Heat Transfer and Fluid Flow*, Hemisphere Publishing Corp., 1980, pp. 52–54.

14. Mack, B.L., 1991, "Natural Convection From an Isothermal Cube on a Vertical Plate," M.A.Sc. Thesis, University of Waterloo, Waterloo, Canada.

15. Incropera, F.P., Dewitt, D.P., *Fundamentals of Heat and Mass Transfer*, 3rd ed. John Wiley & Sons, Inc., 1990, New York, pp. A3.

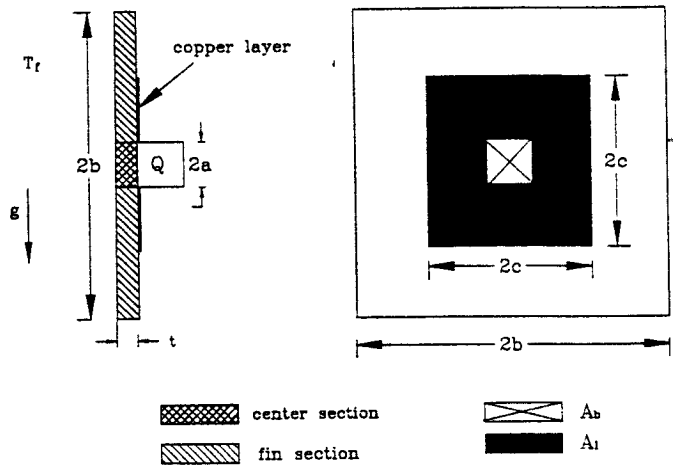

Figure 1: Configuration of Cube on Plate Assembly

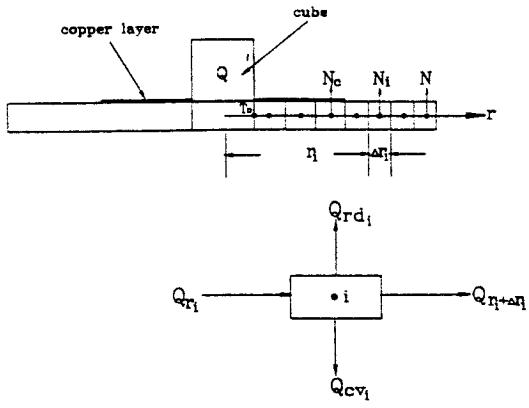

Figure 2: Control Volumes of Fin Section

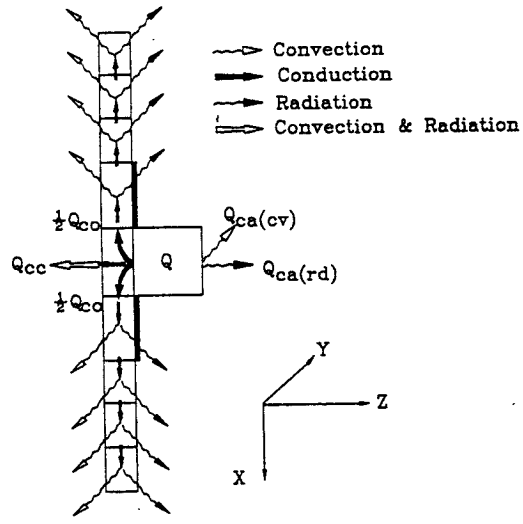

Figure 3: Heat Dissipation from the Cubic Heat Source and the Plate

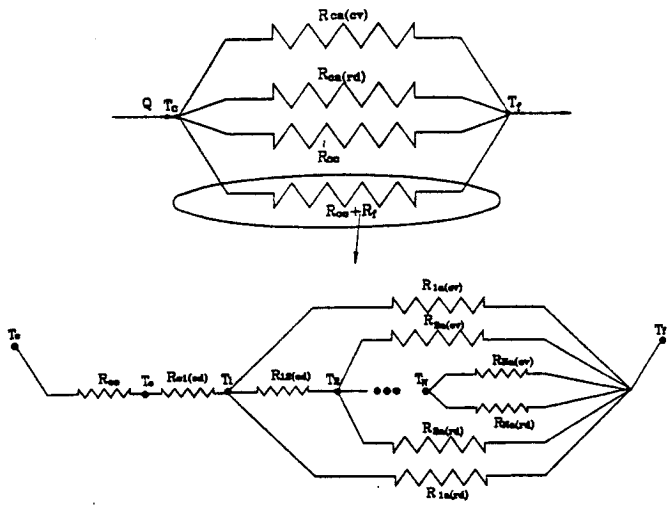

Figure 4: Thermal Resistance Network of Cube-on-Plate Assembly

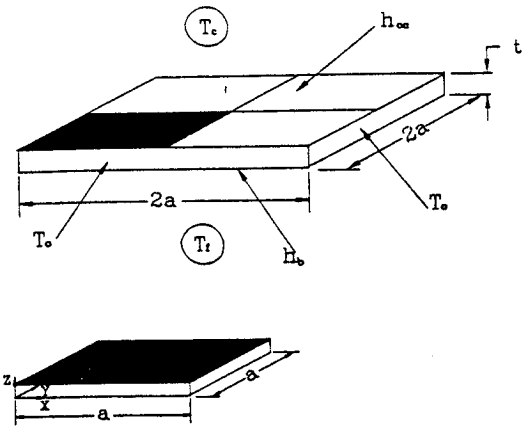

Figure 5: Coordinate System, Dimensions and Boundary Conditions of the Center Section

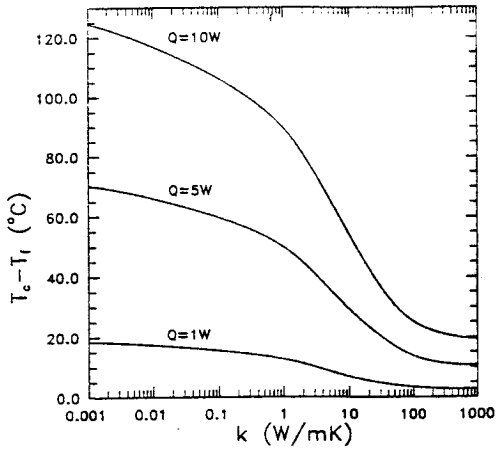

Figure 6: Effect of Plate Thermal Conductivity on Cube Temperature Excess

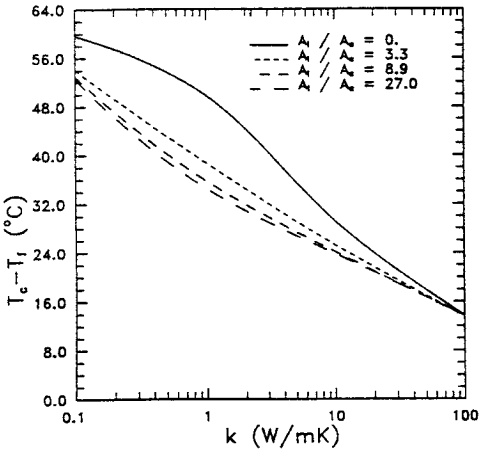

Figure 7: Effect of Copper Layer on Cube Temperature Excess

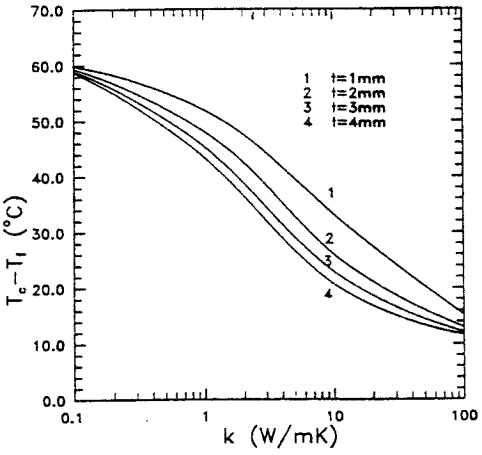

Figure 8: Effect of Plate Thickness on Cube Temperature Excess

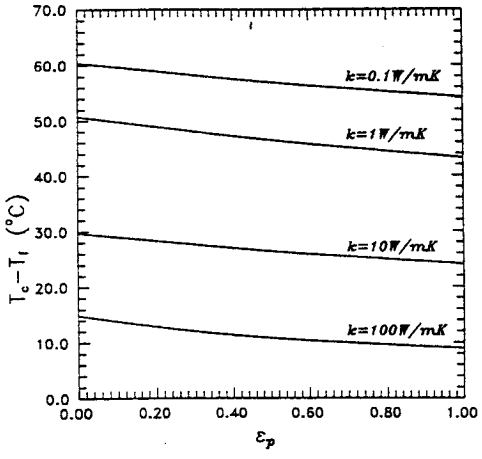

Figure 9: Effect of Plate Emissivity on Cube Temperature Excess

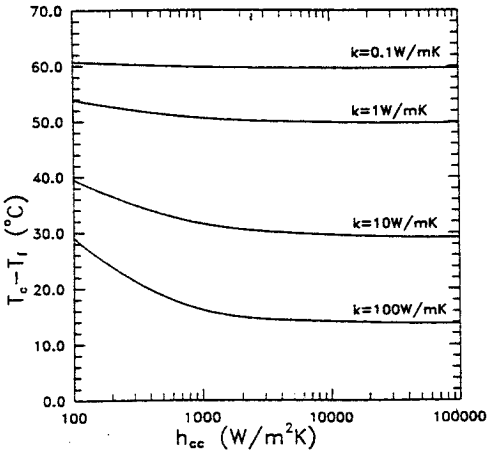

Figure 10: Effect of Contact Resistance on Cube Temperature Excess

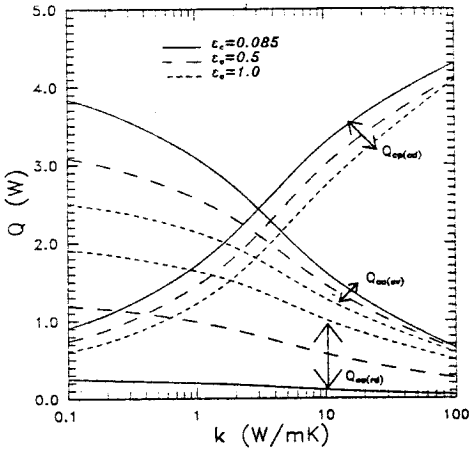

Figure 11: Relative Fraction of Heat Dissipation from the Cube

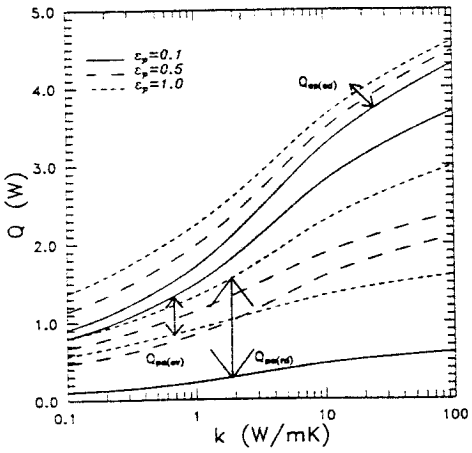

Figure 12: Relative Fraction of Heat Dissipation from the Plate

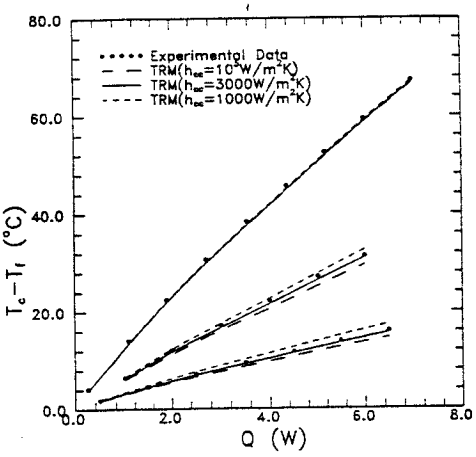

Figure 13: Experiment vs Predicted Results for Case 1A—1C

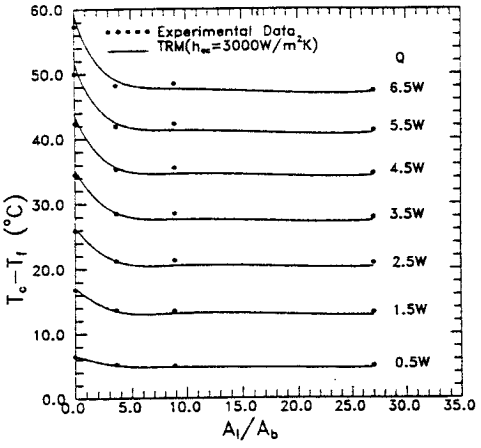

Figure 14: Experiment vs Predicted Results for Cases 2A—2D